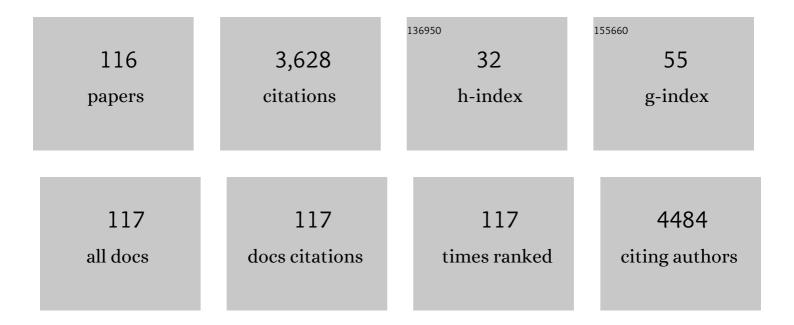
Xiaoling Zhang

List of Publications by Year in descending order

Source: https://exaly.com/author-pdf/3359170/publications.pdf Version: 2024-02-01



#	Article	IF	CITATIONS
1	A 4-hydroxynaphthalimide-derived ratiometric fluorescent chemodosimeter for imaging palladium in living cells. Chemical Communications, 2011, 47, 8656.	4.1	230
2	A highly selective colorimetric and ratiometric fluorescent chemodosimeter for imaging fluoride ions in living cells. Chemical Communications, 2011, 47, 7098.	4.1	173
3	Atomic Iron Catalysis of Polysulfide Conversion in Lithium–Sulfur Batteries. ACS Applied Materials & Interfaces, 2018, 10, 19311-19317.	8.0	152
4	Turn-on theranostic fluorescent nanoprobe by electrostatic self-assembly of carbon dots with doxorubicin for targeted cancer cell imaging, in vivo hyaluronidase analysis, and targeted drug delivery. Biosensors and Bioelectronics, 2017, 96, 300-307.	10.1	144
5	Rational Design of a Hepatoma-Specific Fluorescent Probe for HOCl and Its Bioimaging Applications in Living HepG2 Cells. Analytical Chemistry, 2019, 91, 2163-2168.	6.5	107
6	A lysosome targetable versatile fluorescent probe for imaging viscosity and peroxynitrite with different fluorescence signals in living cells. Journal of Materials Chemistry B, 2018, 6, 580-585.	5.8	104
7	An Endoplasmic Reticulum-Targeted Ratiometric Fluorescent Probe for the Sensing of Hydrogen Sulfide in Living Cells and Zebrafish. Analytical Chemistry, 2020, 92, 9982-9988.	6.5	103
8	Endoplasmic Reticulum-Directed Ratiometric Fluorescent Probe for Quantitive Detection of Basal H ₂ O ₂ . Analytical Chemistry, 2017, 89, 12945-12950.	6.5	101
9	Highly luminescent, biocompatible ytterbium(<scp>iii</scp>) complexes as near-infrared fluorophores for living cell imaging. Chemical Science, 2018, 9, 3742-3753.	7.4	101
10	A fast-response, highly sensitive and selective fluorescent probe for the ratiometric imaging of nitroxyl in living cells. Chemical Communications, 2014, 50, 6013.	4.1	97
11	16.5% efficiency ternary organic photovoltaics with two polymer donors by optimizing molecular arrangement and phase separation. Nano Energy, 2020, 69, 104447.	16.0	80
12	Construction of an orthogonal ZnSalen/Salophen library as a colour palette for one- and two-photon live cell imaging. Chemical Science, 2014, 5, 2318.	7.4	66
13	Synthesis of N-Doped Micropore Carbon Quantum Dots with High Quantum Yield and Dual-Wavelength Photoluminescence Emission from Biomass for Cellular Imaging. Nanomaterials, 2019, 9, 495.	4.1	65
14	A highly sensitive and rapidly responding fluorescent probe with a large Stokes shift for imaging intracellular hypochlorite. Sensors and Actuators B: Chemical, 2016, 236, 459-465.	7.8	58
15	Rational design of ZnSalen as a single and two photon activatable fluorophore in living cells. Chemical Science, 2012, 3, 3315.	7.4	57
16	A mitochondria targetable and viscosity sensitive fluorescent probe and its applications for distinguishing cancerous cells. Dyes and Pigments, 2019, 168, 134-139.	3.7	53
17	Unravelling the correlation between metal induced aggregation and cellular uptake/subcellular localization of Znsalen: an overlooked rule for design of luminescent metal probes. Chemical Science, 2015, 6, 2389-2397.	7.4	52
18	Stable DNA Nanomachine Based on Duplex–Triplex Transition for Ratiometric Imaging Instantaneous pH Changes in Living Cells. Analytical Chemistry, 2015, 87, 5854-5859.	6.5	51

#	Article	IF	CITATIONS
19	Combining myeloperoxidase (MPO) with fluorogenic ZnSalen to detect lysosomal hydrogen peroxide in live cells. Chemical Science, 2013, 4, 2947.	7.4	49
20	An ultrafast responsive BODIPY-based fluorescent probe for the detection of endogenous hypochlorite in live cells. Journal of Materials Chemistry B, 2017, 5, 525-530.	5.8	49
21	A fluorescent probe for differentiating Cys, Hcy and GSH via a stepwise interaction. Sensors and Actuators B: Chemical, 2018, 262, 345-349.	7.8	49
22	A reversible water-soluble naphthalimide-based chemosensor for imaging of cellular copper(II) ion and cysteine. Sensors and Actuators B: Chemical, 2018, 256, 632-638.	7.8	45
23	A mitochondria-targeting highly specific fluorescent probe for fast sensing of endogenous peroxynitrite in living cells. Sensors and Actuators B: Chemical, 2020, 303, 127284.	7.8	45
24	A fast-response, highly sensitive and selective fluorescent probe for the ratiometric imaging of hydrogen peroxide with a 100 nm red-shifted emission. RSC Advances, 2014, 4, 16055.	3.6	42
25	Reversible and Dynamic Fluorescence Imaging of Cellular Redox Self-Regulation Using Fast-Responsive Near-Infrared Ge-Pyronines. ACS Applied Materials & Interfaces, 2016, 8, 8991-8997.	8.0	41
26	Rational design of aggregation-induced emission sensor based on Rhodamine B for turn-on sensing of trivalent metal cations, reversible data protection, and bioimaging. Materials Chemistry Frontiers, 2019, 3, 151-160.	5.9	41
27	Donor–acceptor type aggregation-induced emission luminophores based on the 1,1-dicyanomethylene-3-indanone unit for bridge-dependent reversible mechanochromism and light-up biosensing of hypochlorites. Journal of Materials Chemistry C, 2019, 7, 8888-8897.	5.5	40
28	An ICT-based fluorescent probe for ratiometric monitoring the fluctuations of peroxynitrite in mitochondria. Sensors and Actuators B: Chemical, 2021, 328, 129069.	7.8	37
29	A near-infrared fluorescent probe for ratiometric imaging peroxynitrite in Parkinson's disease model. Sensors and Actuators B: Chemical, 2022, 359, 131393.	7.8	37
30	Dual-Site Fluorescent Probe to Monitor Intracellular Nitroxyl and GSH-GSSG Oscillations. Analytical Chemistry, 2019, 91, 4451-4456.	6.5	36
31	A mitochondria-targeted far red fluorescent probe for ratiometric imaging of endogenous peroxynitrite. Dyes and Pigments, 2019, 170, 107609.	3.7	35
32	An AlEgen-based fluorescent probe for highly selective and specific imaging of lipid droplets in LO2 and HepG2 cells. Sensors and Actuators B: Chemical, 2019, 284, 545-552.	7.8	35
33	In Vitro Lightâ€Up Visualization of a Subunitâ€Specific Enzyme by an AIE Probe via Restriction of Single Molecular Motion. Angewandte Chemie - International Edition, 2020, 59, 10003-10007.	13.8	34
34	β-Lactonization of fluorinated porphyrin enhances LDL binding affinity, cellular uptake with selective intracellular localization. Chemical Science, 2014, 5, 558-566.	7.4	33
35	A sensitive ratiometric fluorescent probe for quantitive detection and imaging of alkaline phosphatase in living cells. Analytica Chimica Acta, 2019, 1066, 131-135.	5.4	33
36	A conformational transition based fluorescent probe for mapping lysosomal viscosity fluctuations by fluorescence lifetime imaging. Sensors and Actuators B: Chemical, 2021, 331, 129432.	7.8	33

#	Article	IF	CITATIONS
37	A highly selective colorimetric and far-red fluorescent probe for imaging bisulfite in living cells. RSC Advances, 2014, 4, 33507.	3.6	32
38	Enantioselective Fluorescent Imaging of Free Amino Acids in Living Cells. Chemistry - A European Journal, 2017, 23, 2432-2438.	3.3	32
39	Highly Sensitive and Selective Detection of Heparin in Serum Based on a Long-Wavelength Tetraphenylethylene–Cyanopyridine Aggregation-Induced Emission Luminogen. Analytical Chemistry, 2020, 92, 7106-7113.	6.5	32
40	Ratiometric fluorescence imaging of endogenous selenocysteine in cancer cell matrix. Journal of Materials Chemistry B, 2017, 5, 6890-6896.	5.8	31
41	One-Pot Synthesis of Hollow PbSe Single-Crystalline Nanoboxes via Gas Bubble Assisted Ostwald Ripening. Crystal Growth and Design, 2010, 10, 1257-1262.	3.0	30
42	A highly sensitive and reductant-resistant fluorescent chemodosimeter for the rapid detection of nitroxyl. Sensors and Actuators B: Chemical, 2015, 220, 727-733.	7.8	30
43	A Chloroacetateâ€Caged Fluorescein Chemodosimeter for Imaging Cysteine/Homocysteine in Living Cells. European Journal of Organic Chemistry, 2013, 2013, 888-893.	2.4	29
44	A reductant-resistant ratiometric, colorimetric and far-red fluorescent probe for rapid and ultrasensitive detection of nitroxyl. Journal of Materials Chemistry B, 2017, 5, 3557-3564.	5.8	29
45	A two-photon fluorescent probe for basal formaldehyde imaging in zebrafish and visualization of mitochondrial damage induced by FA stress. Analyst, The, 2019, 144, 2297-2303.	3.5	29
46	Revealing the redox status in endoplasmic reticulum by a selenium fluorescence probe. Journal of Materials Chemistry B, 2020, 8, 2660-2665.	5.8	29
47	Mitochondria-specific ultrasensitive ratiometric AIE probe for imaging endogenous peroxynitrite. Sensors and Actuators B: Chemical, 2021, 344, 130206.	7.8	29
48	UV-assisted synthesis of long-wavelength Si-pyronine fluorescent dyes for real-time and dynamic imaging of glutathione fluctuation in living cells. Journal of Materials Chemistry B, 2016, 4, 4826-4831.	5.8	28
49	Synthesis of Black Phosphorus Quantum Dots with High Quantum Yield by Pulsed Laser Ablation for Cell Bioimaging. Chemistry - an Asian Journal, 2018, 13, 1842-1846.	3.3	28
50	A highly sensitive and selective fluorescent probe for N ₂ H ₄ in air and living cells. New Journal of Chemistry, 2017, 41, 11891-11897.	2.8	27
51	Over 16.5% efficiency in ternary organic solar cells by adding an alloyed acceptor with energy transfer process. Dyes and Pigments, 2021, 192, 109434.	3.7	24
52	One-pot self-assembly of flower-like Cu2S structures with near-infrared photoluminescent properties. CrystEngComm, 2011, 13, 6549.	2.6	22
53	1-Hexadecylamine as both reducing agent and stabilizer to synthesize Au and Ag nanoparticles and their SERS application. Journal of Nanoparticle Research, 2011, 13, 1929-1936.	1.9	22
54	Ionically dispersed Fe(<scp>ii</scp>)–N and Zn(<scp>ii</scp>)–N in porous carbon for acidic oxygen reduction reactions. Chemical Communications, 2017, 53, 11453-11456.	4.1	22

#	Article	IF	CITATIONS
55	Triphenylphosphine-assisted highly sensitive fluorescent chemosensor for ratiometric detection of palladium in solution and living cells. RSC Advances, 2015, 5, 97121-97126.	3.6	21
56	An ESIPT based naphthalimide chemosensor for visualizing endogenous ONOO ^{â^'} in living cells. RSC Advances, 2018, 8, 1826-1832.	3.6	21
57	A deep red ratiometric fluorescent probe for accurate detection of peroxynitrite in mitochondria. Analytica Chimica Acta, 2022, 1203, 339652.	5.4	21
58	A two-photon fluorescent probe for imaging of endogenous formaldehyde in HeLa cells and quantitative detection of basal formaldehyde in milk samples. Analytical Methods, 2019, 11, 2969-2975.	2.7	20
59	A multifunctional oxygen-producing MnO ₂ -based nanoplatform for tumor microenvironment-activated imaging and combination therapy <i>in vitro</i> . Journal of Materials Chemistry B, 2020, 8, 9943-9950.	5.8	20
60	Hierarchical design of nitrogen-doped porous carbon nanorods for use in high efficiency capacitive energy storage. RSC Advances, 2017, 7, 22447-22453.	3.6	19
61	Porous carbon electrocatalyst with exclusive metal-coordinate active sites for acidic oxygen reduction reaction. Carbon, 2018, 132, 85-94.	10.3	19
62	A ratiometric fluorescent probe for mitochondrial esterase specific detection in living cells. Dyes and Pigments, 2020, 178, 108345.	3.7	19
63	Advances in aptamers against Al² and applications in Al² detection and regulation for Alzheimer's disease. Theranostics, 2022, 12, 2095-2114.	10.0	18
64	Surfactant-sensitized ratiometric fluorescent chemodosimeter for the highly selective detection of mercury(ii) ions based on vinyl ether oxymercuration. RSC Advances, 2014, 4, 12596.	3.6	17
65	Enantioselective Fluorescent Recognition of Amino Acids by Amide Formation: An Unusual Concentration Effect. Journal of Organic Chemistry, 2017, 82, 12669-12673.	3.2	17
66	Mitochondrial directed ratiometric fluorescent probe for quantitive detection of sulfur dioxide derivatives. New Journal of Chemistry, 2019, 43, 5255-5259.	2.8	17
67	Tumor Microenvironment-Responsive Theranostic Nanoplatform for in Situ Self-Boosting Combined Phototherapy through Intracellular Reassembly. ACS Applied Materials & Interfaces, 2020, 12, 6966-6977.	8.0	17
68	A simple dual-response fluorescent probe for imaging of viscosity and ONOOâ^' through different fluorescence signals in living cells and zebrafish. Spectrochimica Acta - Part A: Molecular and Biomolecular Spectroscopy, 2021, 260, 119990.	3.9	17
69	A real-time ratiometric fluorescent probe for imaging of SO ₂ derivatives in mitochondria of living cells. RSC Advances, 2019, 9, 22348-22354.	3.6	16
70	Multimodal Nanoprobe for Pancreatic Beta Cell Detection and Amyloidosis Mitigation. Chemistry of Materials, 2020, 32, 1080-1088.	6.7	16
71	An ESIPT-based fluorescent probe with large Stokes shift for peroxynitrite detection in HeLa cells and zebrafish. Dyes and Pigments, 2022, 204, 110334.	3.7	15
72	Highly specific and ratiometric fluorescent probe for ozone assay in indoor air and living cells. Dyes and Pigments, 2016, 127, 67-72.	3.7	14

#	Article	IF	CITATIONS
73	Fluorescence imaging of lysosomal hydrogen selenide under oxygen-controlled conditions. Journal of Materials Chemistry B, 2019, 7, 2829-2834.	5.8	14
74	A thiocarbonate-caged fluorescent probe for specific visualization of peroxynitrite in living cells and zebrafish. Analyst, The, 2021, 146, 7627-7634.	3.5	14
75	Fluorescence enhancement of acridine orange in a water solution by Au nanoparticles. Science China: Physics, Mechanics and Astronomy, 2010, 53, 1799-1804.	5.1	13
76	Mn-doped CdS/ZnS/CdS QD-based fluorescent nanosensor for rapid, selective, and ultrasensitive detection of copper(<scp>ii</scp>) ion. RSC Advances, 2015, 5, 63458-63464.	3.6	13
77	Synergistic Doping for Pseudocapacitance Sites in Alkaline Carbon Supercapacitors. ChemElectroChem, 2018, 5, 84-92.	3.4	13
78	A fast-responding, highly sensitive detection system consisting of a fluorescent probe and palladium ions for N ₂ H ₄ in environmental water and living cells. Analytical Methods, 2019, 11, 5023-5030.	2.7	13
79	Ratiometric fluorescence imaging for sodium selenite in living cells. Dyes and Pigments, 2019, 164, 133-138.	3.7	12
80	Template synthesis of silver indium sulfide based nanocrystals performed through cation exchange in organic and aqueous media. Nano Research, 2021, 14, 2321.	10.4	12
81	One-step G-quadruplex-based fluorescence resonance energy transfer sensing method for ratiometric detection of uracil-DNA glycosylase activity. Talanta, 2021, 221, 121609.	5.5	12
82	Specific and sensitive imaging of basal cysteine over homocysteine in living cells. RSC Advances, 2018, 8, 37410-37416.	3.6	11
83	A highly colorimetric and ratiometric fluorescent probe for the detection of fluoride ions using test strips. Analytical Methods, 2019, 11, 3844-3850.	2.7	11
84	Enhanced Enantioselectivity in the Fluorescent Recognition of a Chiral Diamine by Using a Bisbinaphthyl Dialdehyde. ACS Omega, 2018, 3, 12545-12548.	3.5	10
85	Synergistic toughening of nanocomposite hydrogel based on ultrasmall aluminum hydroxide nanoparticles and hydroxyapatite nanoparticles. Polymer Composites, 2019, 40, 942-951.	4.6	9
86	Solid-state emissive O-BODIPY dyes with bimodal emissions across red and near infrared region. RSC Advances, 2019, 9, 16246-16251.	3.6	8
87	Ratiometric fluorescent probe for highly selective detection of gaseous H2Se. Dyes and Pigments, 2020, 177, 108274.	3.7	8
88	Defective Ag–In–S/ZnS quantum dots: an oxygen-derived free radical scavenger for mitigating macrophage inflammation. Journal of Materials Chemistry B, 2021, 9, 8971-8979.	5.8	8
89	Effects of reaction temperature on size and optical properties of CdSe nanocrystals. Bulletin of Materials Science, 2010, 33, 547-552.	1.7	7
90	A dual-functional biomimetic-mineralized nanoplatform for glucose detection and therapy with cancer cells <i>in vitro</i> . Journal of Materials Chemistry B, 2021, 9, 3885-3891.	5.8	7

#	Article	IF	CITATIONS
91	An efficient FRET based theranostic nanoprobe for hyaluronidase detection and cancer therapy in vitro. Sensors and Actuators B: Chemical, 2021, 344, 130201.	7.8	7
92	An electrostatically regulated organic self-assembly for rapid and sensitive detection of heparin in serum. Analytical Methods, 2021, 13, 3620-3626.	2.7	7
93	Selfâ€Assembled Monomolecular Layer Modified ZnO for Efficient Inverted Polymer Solar Cells with 11.53% Efficiency. Physica Status Solidi - Rapid Research Letters, 2019, 13, 1900372.	2.4	6
94	A fluorescent probe based on reversible Michael addition–elimination reaction for the cycle between cysteine and H ₂ O ₂ . Analytical Methods, 2020, 12, 3797-3801.	2.7	6
95	In Vitro Lightâ€Up Visualization of a Subunitâ€Specific Enzyme by an AIE Probe via Restriction of Single Molecular Motion. Angewandte Chemie, 2020, 132, 10089-10093.	2.0	6
96	Novel bimetallic Cu/Ni core-shell NPs and nitrogen doped GQDs composites applied in glucose in vitro detection. PLoS ONE, 2019, 14, e0220005.	2.5	5
97	Reaction rate constants with OH radicals at 253–328—K and atmospheric implications for (CF3)2CHOCxH(2xâ€~+â€~1) (xâ€=â€~1, 2, 3). Chemical Physics Letters, 2019, 714, 125-130.	2.6	5
98	Off–On Squalene Epoxidase-Specific Fluorescent Probe for Fast Imaging in Living Cells. Analytical Chemistry, 2021, 93, 14716-14721.	6.5	5
99	On the fluorescence of C60 at room temperature. Science China: Physics, Mechanics and Astronomy, 2010, 53, 95-99.	5.1	4
100	Aqueous nanodispersion of acetylene tethered, quinoxaline-containing conjugated polymer as fluorescence probe for Ag+. New Journal of Chemistry, 2014, 38, 4730-4735.	2.8	4
101	A label-free ratiometric fluorescence strategy for 3′–5′ exonuclease detection. New Journal of Chemistry, 2018, 42, 16630-16634.	2.8	4
102	An analytical method for overlapping of the melting and decomposition of 2-oximemalononitrile. Journal of Thermal Analysis and Calorimetry, 2020, , 1.	3.6	4
103	A Sensitive Fluorescent Probe for Homocysteine/Cysteine in Pure Aqueous Media and Mitochondria. ChemistrySelect, 2021, 6, 8391-8396.	1.5	4
104	A silicon nanoparticle-based nanoprobe for ratiometric fluorescence and visual detection of glucose. New Journal of Chemistry, 2021, 45, 19515-19520.	2.8	4
105	Evaluation of the Thermal Hazard of the Oxidation Reaction in the Synthesis of 3,4-Bis(4-nitrofurazan-3-yl)furoxan. Organic Process Research and Development, 2022, 26, 1389-1397.	2.7	4
106	A Multiâ€crosslinking Nanocapsuleâ€Based Serialâ€Stimuliâ€Responsive Leakageâ€Free Drugâ€Delivery System Vitro. Chemistry - A European Journal, 2019, 25, 13017-13024.	In 3.3	3
107	A novel vapor-phase catalytic synthetic approach for industrial production of 1,1,1,3,3,3-hexafluoroisopropyl methylether. Applied Catalysis A: General, 2020, 594, 117416.	4.3	3
108	Polydopamine nanodots-based cost-effective nanoprobe for glucose detection and intracellular imaging. Analytical and Bioanalytical Chemistry, 2021, 413, 4865-4872.	3.7	3

#	Article	IF	CITATIONS
109	Enhanced Performance of Carbonâ€Based, Fully Printed Mesoscopic Perovskite Solar Cells through Defects Passivation. Advanced Materials Interfaces, 2022, 9, .	3.7	3
110	A xanthene-based fluorescent probe for detection of peroxynitrite in living cells and zebrafish. Spectrochimica Acta - Part A: Molecular and Biomolecular Spectroscopy, 2022, 277, 121264.	3.9	3
111	Synthesis of SERS active Au nanowires in different noncoordinating solvents. Journal of Nanoparticle Research, 2011, 13, 2625-2632.	1.9	2
112	One-step synthesis of PY-NBD to distinguish Cys/Hcy and GSH in aqueous solutions and living cells by dual channels. New Journal of Chemistry, 2022, 46, 6715-6719.	2.8	2
113	Enzyme-triggered DNA nanomimosa: A ratiometric nanoprobe for RNase H activity sensing in living cells. Talanta, 2021, 233, 122547.	5.5	1
114	Surfaceâ€enhanced Raman spectroscopy coupled with advanced chemometric models for quantification of sulfide anion in environmental water samples. Journal of Raman Spectroscopy, 2022, 53, 202-210.	2.5	1
115	Vapor-phase catalytic methylation of 1,1,1,3,3,3-hexafluoroisopropanol for the mass production of 1,1,1,3,3,3-hexafluoroisopropyl methyl ether. Journal of Fluorine Chemistry, 2021, 241, 109673.	1.7	0
116	Electrical properties of carbon-based fully-printed mesoscopic perovskite solar cells with BAI as an additive. Journal of Materials Science: Materials in Electronics, 2022, 33, 3091-3100.	2.2	0